Analytical solution of electro-osmotic flow in a semicircular microchannel

Chang-Yi Wang,[1,2] Ying-Hong Liu,[1,3] and Chien C. Chang[1,3,a)]
[1]*Division of Mechanics, Research Center for Applied Sciences, Academia Sinica, Taipei 115, Taiwan, Republic of China*
[2]*Departments of Mathematics and Mechanical Engineering, Michigan State University, East Lansing, Michigan 48824, USA*
[3]*Institute of Applied Mechanics and Taida Institute of Mathematical Sciences, National Taiwan University, Taipei 106, Taiwan, Republic of China*

(Received 7 January 2008; accepted 13 May 2008; published online 25 June 2008)

The electro-osmotic flow through a microchannel with a semicircular cross section is studied under the Debye–Huckel approximation. Analytical series solutions are found for two basic cases. The solutions for the two basic cases considered can be superposed to yield solutions for any combination of constant zeta potentials on the flat or curved wall boundaries. Moreover, in the limit of a thin electric double layer (small Debye length compared to the nominal dimension), a method of solution is shown for variable zeta potentials by using the Smoluchowski slip approximation. © *2008 American Institute of Physics*. [DOI: 10.1063/1.2939399]

I. INTRODUCTION

Microfluidic devices have become important due to their applications in microelectromechanical systems and microbiological sensors such as laboratory on a chip.[1,2] One way to transport fluids through microtubes without mechanical moving parts is to utilize electro-osmosis (EO) (see, e.g., Ref. 3). The principle is as follows. Most solid surfaces carry a negative electrostatic charge when in contact with a fluid containing dissociated salts. At the same time, the fluid acquires a positive charge near the boundary. The charged fluid can then be moved by an applied axial electric field.

For parallel steady flow caused solely by EO in a tube, the fluid velocity is governed by the reduced Navier–Stokes equation

$$\nabla^2 w = -\rho_e E/\mu, \tag{1}$$

where w is the longitudinal fluid velocity, μ is the fluid viscosity, E is the longitudinal applied electric field, and ρ_e is the charge density which can be expressed by a potential distribution ψ,

$$\rho_e = -\varepsilon\nabla^2\psi = -2zen_0 \sinh\left(\frac{ze\psi}{k_BT}\right). \tag{2}$$

Here ε is the electric permittivity of the medium, e is the electron charge, n_0 is the bulk electrolyte concentration of a binary electrolyte dissociating into cations and anions of valence z, k_B is the Boltzmann constant, and T is the temperature. Equation (2) is the nonlinear Poisson–Boltzmann equation. The boundary condition is that the velocity is zero and the zeta potential ψ_0 is given on the wall of the channel, or, more precisely on the Stern plane.[3]

If the electrical potential is small compared to the thermal energy of ions, the ratio $(ze\psi_0/k_BT)$ is much less than 1. Let $\phi=\psi/\psi_0$ (where ψ_0 can be taken to the maximum zeta potential) and normalize all the lengths by the radius of the semicircle, L. Equation (2), under the Debye–Huckel approximation, is linearized to

$$\nabla_0^2\phi = K^2\phi, \tag{3}$$

where we have the normalized Laplace operator $L^2\nabla^2=\nabla_0^2=\partial^2/\partial x^2+\partial^2/\partial y^2$, with x and y the normalized Cartesian coordinates, and have defined $K^2=(\kappa L)^2=2z^2e^2n_0L^2/(\varepsilon k_BT)$. K is called the nondimensional electrokinetic width, and κ is the Debye–Huckel parameter and its inverse is called the Debye length.

If we normalize velocity by $u=-w/(\varepsilon E\psi_0/\mu)$, Eq. (1) becomes

$$\nabla_0^2 u = -\nabla_0^2\phi = -K^2\phi. \tag{4}$$

Analytical solutions to Eq. (3) and the resulting flow for the parallel channel can be written in terms of exponential functions. The circular cross section was solved by Rice and Whitehead[4] using modified Bessel functions and extended to annular flows by Tsao.[5] The solutions for the rectangular cross section can be expressed in double infinite series.[6] For all other cross sections, numerical methods such as finite elements or boundary collocation[7,8] must be used.

The purpose of the present paper is to present an analytical solution for the EO flow in a semicircular microchannel. Analytical solutions are rare. Not only do they represent EO flows through fundamental cross sectional shapes but they also serve as standards for asymptotic and fully numerical methods.

II. ANALYSIS

Figure 1(a) shows a semicircular cross section of width $2L$. The flat wall has constant electric potential ψ_0 which may be different from the constant electric potential ψ_0' on the curved wall. The problem can be separated into two basic problems, each with zero potential on one wall [Figs. 1(b) and 1(c)] where we have appropriately normalized the potentials with ψ_0 or ψ_0'.

a)Author to whom correspondence should be addressed. Telephone: 886-2-33665671. FAX: 886-2-23625238. Electronic mail: mechang@gate.sinica.edu.tw.

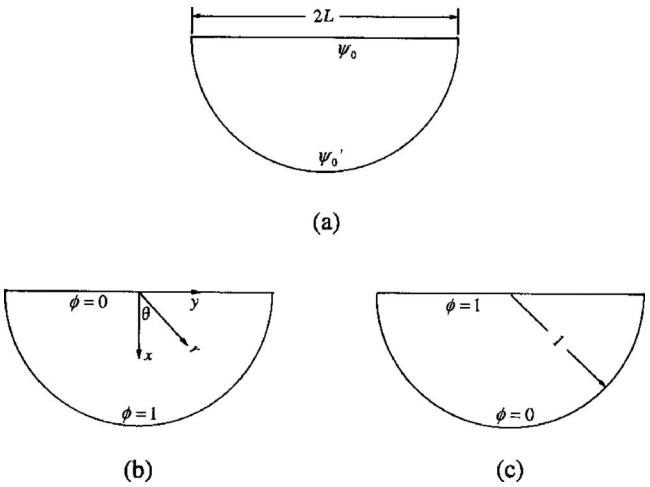

FIG. 1. (a) The semicircular channel with different constant zeta potentials on the boundaries. (b) Case A: The normalized problem with zero potential on the flat wall boundary. (c) Case B: The problem with zero potential on the curved wall boundary.

For case A [Fig. 1(b)], the normalized zeta potential is zero on the flat wall and unity on the circular wall. The bounded solution to Eq. (3) which is zero on the flat wall is

$$\phi = \sum_{n=1}^{\infty} a_n I_{\lambda_n}(Kr)\cos(\lambda_n\theta), \tag{5}$$

where (r,θ) are cylindrical coordinates, a_n are coefficients to be determined, I is the modified Bessel function, and $\lambda_n \equiv 2n-1$. The boundary condition on the curved wall $r=1$ is then applied,

$$1 = \sum_{n=1}^{\infty} a_n I_{\lambda_n}(K)\cos(\lambda_n\theta). \tag{6}$$

A Fourier inversion gives

$$a_n = \frac{4(-1)^{n+1}}{\pi\lambda_n I_{\lambda_n}(K)}. \tag{7}$$

For the velocity, we note from Eq. (4) that a particular solution is $u=-\phi$. The general solution which satisfies zero velocity on the flat wall is

$$u = \sum_{n=1}^{\infty} b_n r^{\lambda_n}\cos(\lambda_n\theta) - \phi. \tag{8}$$

Zero velocity on $r=1$ gives

$$0 = \sum_{n=1}^{\infty} b_n \cos(\lambda_n\theta) - 1 \tag{9}$$

or

$$b_n = \frac{4(-1)^{n+1}}{\pi\lambda_n}. \tag{10}$$

Thus the velocity distribution is

TABLE I. The value of Q for various K as the number of terms in the series N.

$N\backslash K$	0.1	1	10	100
1	0.000 424	0.0398	0.0689	0.824
2	0.000 434	0.0408	0.0640	0.877
3	0.000 436	0.0410	0.0646	0.891
4	0.000 436	0.0410	0.0648	0.896
5			0.0649	0.899
6			0.0649	0.900
7				0.901
8				0.901

$$u = \sum_{n=1}^{\infty} \frac{4(-1)^{n+1}}{\pi\lambda_n}\left[r^{\lambda_n} - \frac{I_{\lambda_n}(Kr)}{I_{\lambda_n}(K)}\right]\cos(\lambda_n\theta). \tag{11}$$

The flow rate, normalized by $(\varepsilon E\psi_0' L^2/\mu)$, is

$$Q = 2\int_0^{\pi/2}\int_0^1 urdrd\theta = \frac{8}{\pi}\sum_1^{\infty}\frac{1}{\lambda_n^2}\left(\frac{1}{\lambda_n+2} - H(n,K)\right), \tag{12}$$

where the integral

$$H(n,K) = \int_0^1 \frac{I_{\lambda_n}(Kr)}{I_{\lambda_n}(K)} rdr \tag{13}$$

is given in the Appendix. If the infinite series is truncated to N terms, the value of Q is as shown in Table I. We see that the convergence is fairly fast. For all ranges of K, only ten terms are needed for three-digit accuracy.

For case B [Fig. 1(c)], the normalized zeta potential is unity on the flat wall and zero on the circular wall. A combination of Cartesian and cylindrical coordinates is used. The solution to Eq. (3) which is unity on the flat wall is

$$\phi = e^{-Kx} + \sum_1^{\infty} a_n I_{\lambda_n}(Kr)\cos(\lambda_n\theta). \tag{14}$$

Here (x,y) are Cartesian coordinates and the exponential term reflects the decay characteristic of the electric potential from the charged boundary. The boundary condition on the curved boundary gives

$$0 = e^{-K\cos\theta} + \sum_1^{\infty} a_n I_{\lambda_n}(K)\cos(\lambda_n\theta). \tag{15}$$

Inversion yields

$$a_n = -\frac{4G(n,K)}{\pi I_{\lambda_n}(K)}, \tag{16}$$

where the integral

$$G(n,K) = \int_0^{\pi/2} e^{-K\cos\theta}\cos(\lambda_n\theta)d\theta \tag{17}$$

is given in the Appendix. The velocity which is zero on the flat wall is

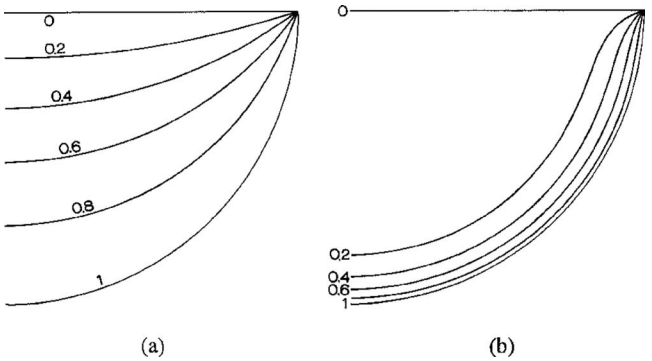

FIG. 2. The potential distribution ϕ when there is no charge on the flat wall boundary: (a) $K=0.1$; (b) $K=10$.

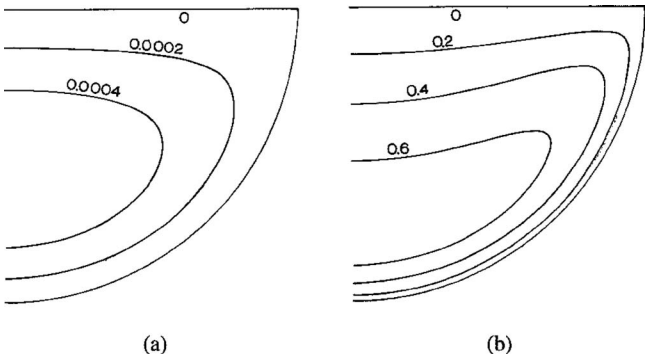

FIG. 3. The velocity distribution u when there is no charge on the flat wall boundary: (a) $K=0.1$, maximum velocity of 0.000 583; (b) $K=10$, maximum velocity of 0.724.

$$u = 1 - \phi + \sum_{1}^{\infty} b_n r^{\lambda_n} \cos(\lambda_n \theta). \tag{18}$$

Zero velocity at $r=1$ gives

$$0 = 1 + \sum_{1}^{\infty} b_n \cos(\lambda_n \theta), \tag{19}$$

from which we obtain

$$b_n = \frac{4(-1)^n}{\pi \lambda_n}. \tag{20}$$

Thus

$$u = 1 - e^{-Kx} + \sum_{1}^{\infty} \frac{4}{\pi}\left[\frac{(-1)^n}{\lambda_n} r^{\lambda_n} + G(n,K)\frac{I_{\lambda_n}(Kr)}{I_{\lambda_n}(K)}\right]\cos(\lambda_n \theta). \tag{21}$$

Note the area integral of the exponential,

$$2\int_0^1 \int_0^{\sqrt{1-y^2}} e^{-Kx} dx dy = \frac{2}{-K}\left(\int_0^1 e^{-K\sqrt{1-y^2}} dy - 1\right) = \frac{2}{-K}\left(\int_0^{\pi/2} e^{-K\cos s} \cos s ds - 1\right) = \frac{2}{-K}[G(1,K) - 1]. \tag{22}$$

Integrating Eq. (21) gives the flow rate,

$$Q = \frac{\pi}{2} + \frac{2}{K}[G(1,K) - 1] - \frac{8}{\pi}\sum_{1}^{\infty} \frac{1}{\lambda_n}\left[\frac{1}{\lambda_n(\lambda_n + 2)} + (-1)^n G(n,K) H(n,K)\right]. \tag{23}$$

Again the convergence of the infinite series is fast so that ten terms are enough to get three significant digits.

III. RESULTS AND DISCUSSION

Typical potential distributions for the case in Fig. 1(b), where only the curved wall is charged, are shown in Fig. 2. For low K, the electric potential ϕ is almost linearly distributed, while for large K, the potential ϕ is concentrated near the circular wall. The corresponding velocity distributions are shown in Fig. 3. As K is increased, the velocity contours cease to be convex and the maximum velocity moves toward the circular boundary.

Figure 4 shows the normalized flow rate Eq. (12) as a function of K. Using Eq. (A3) for small K, the asymptotic expansion is

$$Q \sim \frac{4K^2}{\pi}\sum_{1}^{\infty} \frac{1}{\lambda_n^2(\lambda_n + 1)(\lambda_n + 2)(\lambda_n + 4)} + O(K^4) = 0.043\,64K^2 + O(K^4). \tag{24}$$

On the other hand, for large K, with the help of series summation formulas,[9] we have

$$Q \sim \frac{8}{\pi}\sum_{1}^{\infty} \frac{1}{\lambda_n^2}\left(\frac{1}{\lambda_n + 2} - \frac{1}{K}\right) + O(K^{-2}) = \frac{\pi}{2} - \frac{2}{\pi} - \frac{\pi}{K} + O(K^{-2}). \tag{25}$$

These approximations compare well to the exact form in their respective ranges of validity (Fig. 4).

Typical potential distributions for the case of Fig. 1(c), where only the flat wall is charged, are shown in Fig. 5. The corresponding velocity distributions are shown in Fig. 6. For

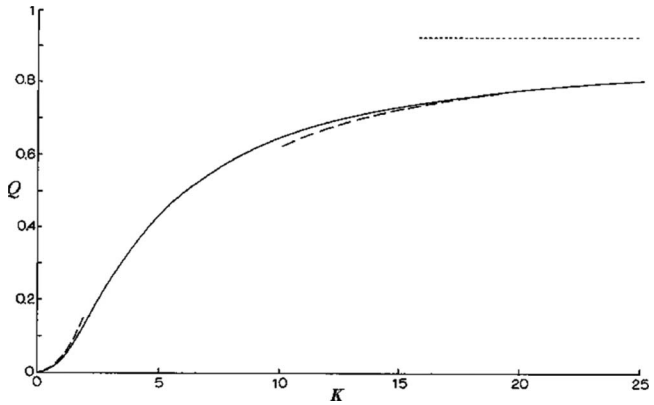

FIG. 4. The flow rate Q vs K when there is no charge on the flat wall boundary. Dashed lines are from Eqs. (24) and (25); dotted line is the asymptote as $K \to \infty$.

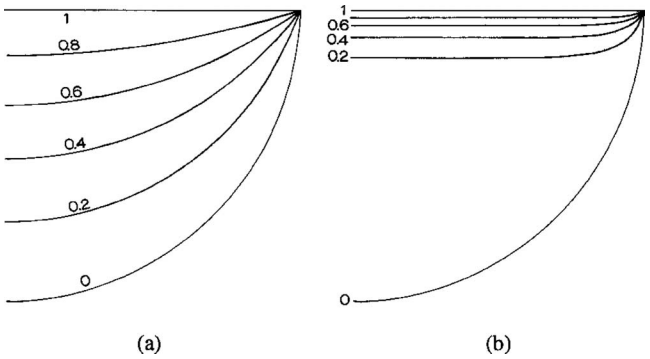

FIG. 5. The potential distribution ϕ when there is no charge on the curved wall boundary: (a) $K=0.1$; (b) $K=10$.

large K, both potential and velocity shift toward the charged flat wall. The flow rate, given by Eq. (23), is plotted in Fig. 7. Note that Fig. 7 is similar to Fig. 4, but not proportional. For large K, the asymptotic form is

$$Q \sim \frac{2}{\pi} - \frac{2}{K} + O(K^{-2}). \tag{26}$$

After some work, the small K expansion is found to be

$$Q \sim \frac{K^2}{\pi}\left[\frac{34}{45} - \frac{\pi^2}{16} - 8\sum_{2}^{\infty}\frac{1}{\lambda_n^2(\lambda_n+2)} \times\left(\frac{1}{\lambda_n^2-4} + \frac{1}{2(\lambda_n+1)(\lambda_n+4)}\right)\right] + O(K^3)$$
$$= 0.030\,75K^2 + O(K^3). \tag{27}$$

These approximations are also shown in Fig. 7.

Finally, for large K, we show how to obtain solution for arbitrary zeta potentials. In the above, we have considered constant zeta potentials on either the flat surface or the curved surface. In the limit of large K, it is possible to obtain a solution for variable zeta potentials on the boundary. The idea is to use the Smoluchowski slip approximation for a thin electric double layer.

For large K, Eq. (3) [and also Figs. 2(b) and 5(b)] shows that an electric double layer of order $1/K$ exists near a charged boundary. Let the layer thickness be much smaller

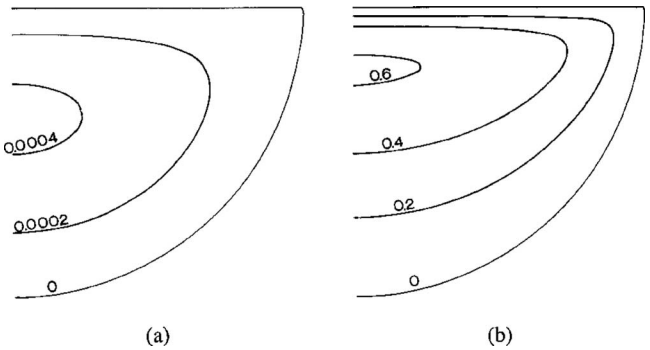

FIG. 6. The velocity distribution u when there is no charge on the curved wall boundary: (a) $K=0.1$, maximum velocity of 0.000 43; (b) $K=10$, maximum velocity of 0.614.

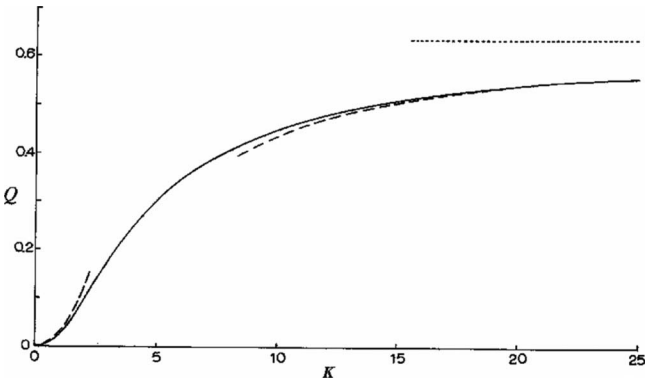

FIG. 7. The flow rate Q vs K when there is no charge on the curved wall boundary. Dashed lines are from Eqs. (26) and (27); dotted line is the asymptote as $K\to\infty$.

than the variable potential scale or the radius of curvature along the boundary, i.e., the normal derivatives are much larger than the tangential derivatives. Let $\phi(x,0)=h(x)$ on a flat surface. Then the solution to Eq. (3) in the electric double layer is essentially

$$\phi = h(x)e^{-Ky}. \tag{28}$$

The velocity in the electric double layer is from Eq. (4),

$$u = h(x)(1-e^{-Ky}). \tag{29}$$

Outside the electric double layer or in the interior, the potential is zero. From Eq. (4) the interior flow satisfies

$$\nabla_0^2 u = 0. \tag{30}$$

The interior velocity is dragged along by the slip velocity u_S, which is obtained from Eq. (29),

$$u_S = h(x). \tag{31}$$

In what follows we shall consider the semicircular channel with high K and nonuniform zeta potentials on the boundary. Separate the problem into two cases: (1) Case A [$\phi=0$ on the flat surface and $\phi=f(\theta)$ on the curved surface, and then $u_S=0$ on the flat surface and $u_S=f(\theta)$ on the curved surface] and (2) case B [$\phi=g(x)$ on the flat surface and $\phi=0$ on the curved surface, and then $u_S=g(x)$ on the flat surface and $u_S=0$ on the curved surface]. Let f and g be symmetrical with respect to their arguments, although these restrictions can be modified. The method is similar to the constant zeta potential cases. Case A is simpler. Expand $f(\theta)$ in a Fourier series as follows:

$$f(\theta) = \sum_{n=1}^{\infty} a_n \cos(\lambda_n\theta), \tag{32}$$

where $\lambda_n=2n-1$. Then the EO velocity that satisfies Eq. (30) and the boundary conditions is

$$u = \sum_{n=0}^{\infty} a_n \cos(\lambda_n\theta) r^{\lambda_n}. \tag{33}$$

For case B, we expand

TABLE II. The values of $H(n,K)$ for various n and K.

$n\backslash K$	0	0.5	1	2	5	10	20	50	100
1	0.3333	0.3292	0.3177	0.2804	0.1715	0.0942	0.0487	0.0198	0.0099
2	0.2000	0.1991	0.1965	0.1869	0.1435	0.0897	0.0481	0.0198	0.0099
3	0.1429	0.1425	0.1416	0.1378	0.1176	0.0827	0.0471	0.0197	0.0099
4	0.1111	0.1110	0.1105	0.1087	0.0979	0.0751	0.0457	0.0196	0.0099
5	0.0909	0.0908	0.0906	0.0895	0.0832	0.0679	0.0440	0.0195	0.0099
6	0.0769	0.0769	0.0767	0.0761	0.0730	0.0614	0.0402	0.0193	0.0099
7	0.0667	0.0666	0.0665	0.0661	0.0634	0.0558	0.0383	0.0191	0.0099
8	0.0588	0.0588	0.0587	0.0584	0.0565	0.0510	0.0365	0.0189	0.0098
9	0.0526	0.0526	0.0526	0.0524	0.0510	0.0468	0.0365	0.0187	0.0098
10	0.0476	0.0476	0.0476	0.0474	0.0464	0.0431	0.0347	0.0185	0.0098

$$g(x) = \sum_{n=1}^{\infty} b_n \cos(\beta_n x), \tag{34}$$

where $\beta_n = (n-1/2)\pi$. Then the EO velocity that satisfies Eq. (30) and the boundary conditions is

$$u = \sum b_n \cos(\beta_n x) e^{-\beta_n y}. \tag{35}$$

However, this solution does not satisfy the zero boundary condition on the curved surface. To cancel the velocity, we use a method similar to case A. Expand

$$\cos(\beta_n \cos\theta) e^{-\beta_n \sin\theta} = \sum_{m=1}^{\infty} c_{nm} \cos(\lambda_m \theta). \tag{36}$$

Then

$$f(\theta) = \sum b_n \sum c_{nm} \cos(\lambda_m \theta). \tag{37}$$

The total solution is thus the difference,

$$u = \sum b_n \cos(\beta_n x) e^{-\beta_n y} - \sum \sum b_n c_{nm} \cos(\lambda_m \theta) r^{\lambda_m}. \tag{38}$$

Note that a_n, b_n, and c_{nm} in Eqs. (32), (34), and (36) are obtained by Fourier inversion. The flow rates for the two separate cases can be readily integrated from Eqs. (33) and (38) over the channel cross section.

IV. CONCLUDING REMARKS

It had not been a trivial task to find analytic solutions for the EO flow through a microchannel even though the linearization under the Debye–Huckel approximation is assumed. The solutions presented here are probably the only analytical solutions aside from parallel plate, circular, annular, and rectangular channels, and the solution singularities at the corners can serve as serious checks for asymptotic and fully numerical methods. Since the equations are linear, the solutions for the two basic cases considered can be superposed to yield solutions for any combination of constant zeta potentials on the flat and curved wall boundaries.

The effects of the nondimensional electrokinetic length K on the normalized flow rate Q have been discussed. The magnitude of K is of order of the ratio of the nominal dimension to the Debye length. In general, for large K (thin electric double layer), boundary layers of both potential and flow are created near the charged wall, while for low K (thick electric double layer), there are no boundary layers. Asymptotic flow rates were derived for small and large K. The EO flow rate increases initially as K^2 and approaches a constant value as $K \to \infty$. The approach is very slow, proportional to $1/K$. A simple analysis for EO flows is to assume a very thin electric double layer or $K \to \infty$. Then the flow rate is maximum Q. Note that the interior velocity is not constant, even for large K, unless the zeta potential is constant on all boundaries. Moreover, in the limit of large K, we showed how to obtain a solution for variable zeta potentials by using the Smoluchowski slip approximation. Since the thickness of the electric double layer is about 10–100 nm, for micron-size channels, the value of K is indeed very large. However, nanosize channels are now being fabricated[10–12] and the analysis for all ranges of K becomes necessary, and one such analysis is now provided by the present study. On the practical side, semicircular channels can be fabricated by etching a groove and covering by a flat plate.

ACKNOWLEDGMENTS

The authors would like to thank one of the referees for suggesting the problem for arbitrary zeta potentials. The work was supported in part by the National Science Council of the Republic of China under Contract Nos. NSC96-2221-E-002-201 and NSC96-2811-E-002-054.

APPENDIX: THE FUNCTIONS $H(n,K)$ AND $G(n,K)$

The integral

$$H(n,K) = \int_0^1 \frac{I_{\lambda_n}(Kr)}{I_{\lambda_n}(K)} r dr \tag{A1}$$

can be written in terms of hypergeometric function F,

$$H(n,K) = \frac{K^{\lambda_n} \Gamma(1+\lambda_n/2)}{2^{\lambda_n+1} I_{\lambda_n}(K)} \times F\left[1+\frac{\lambda_n}{2}, \left\{2+\frac{\lambda_n}{2}, 1+\lambda_n\right\}, \frac{K^2}{4}\right]. \tag{A2}$$

It is, however, more convenient to integrate Eq. (A1) numerically. Table II shows some of the results.

TABLE III. The values of $(-1)^{n+1}G(n,K)$ for various n and K.

$n\backslash K$	0	0.5	1	2	5	10	20	50	100
1	1.0000	0.6796	0.4685	0.2336	0.0459	0.0104	0.0025	0.0004	0.0001
2	0.3333	0.3202	0.2916	0.2242	0.0911	0.0284	0.0074	0.0012	0.0003
3	0.2000	0.1977	0.1912	0.1702	0.0999	0.0406	0.0119	0.0020	0.0005
4	0.1429	0.1421	0.1398	0.1314	0.0941	0.0472	0.0157	0.0028	0.0007
5	0.1111	0.1108	0.1097	0.1057	0.0845	0.0498	0.0188	0.0035	0.0009
6	0.0909	0.0907	0.0901	0.0879	0.0751	0.0497	0.0218	0.0042	0.0011
7	0.0769	0.0768	0.0765	0.0751	0.0669	0.0483	0.0229	0.0049	0.0013
8	0.0667	0.0666	0.0664	0.0655	0.0599	0.0461	0.0240	0.0055	0.0015
9	0.0588	0.0588	0.0586	0.0580	0.0541	0.0436	0.0247	0.0061	0.0017
10	0.0526	0.0526	0.0525	0.0520	0.0492	0.0412	0.0250	0.0067	0.0018

From asymptotic expansions of Bessel functions for small K, we find

$$H \sim \frac{1}{\lambda_n + 2}\left[1 - \frac{K^2}{2(\lambda_n+1)(\lambda_n+4)} + O(K^4)\right]. \tag{A3}$$

This approximation is also valid for moderate K and large n. For large K, we find $H \sim 1/K$ for all n. The integral

$$G(n,K) = \int_0^{\pi/2} e^{-K\cos\theta}\cos(\lambda_n\theta)d\theta \tag{A4}$$

can be expressed in terms of modified Bessel functions $I_n(K)$ and Struve functions $S_n(K)$.[13] For example,

$$G(1,K) = \frac{\pi}{2}[S_{-1}(K) - I_1(K)], \tag{A5}$$

$$G(2,K) = \frac{\pi}{2K^2}[8S_1(K) - 4KS_0(K) + K^2S_{-1}(K) - K^2I_3(K)], \tag{A6}$$

$$\begin{aligned} G(3,K) = \frac{\pi}{2K^3}[&-192S_2(K) + 72KS_1(K) - 12K^2S_0(K) \\ &+ K^3S_{-1}(K) + 12(16+K^2)I_2(K) \\ &- K(48+K^2)I_1(K)], \end{aligned} \tag{A7}$$

etc. Some numerical values are listed in Table III. We see that $G(n,K)$ alternate in sign. For small K,

$$G(1,K) \sim 1 - \frac{\pi}{4}K + \frac{K^2}{3} - \frac{\pi}{32}K^3 + O(K^4), \tag{A8}$$

$$G(n,K) \sim (-1)^{n+1}\left[\frac{1}{\lambda_n} - \frac{K^2}{\lambda_n(\lambda_n^2-4)} + O(K^3)\right], \quad n \neq 1. \tag{A9}$$

For large K, use Watson's lemma to obtain

$$G(n,K) \sim (-1)^{n+1}\left(\frac{\lambda_n}{K^2} - \frac{\lambda_n^3}{K^4} + O(K^{-6})\right). \tag{A10}$$

These expressions are used in the asymptotic expansions for the flow rate.

[1] H. A. Stone, A. D. Stroock, and A. Ajdari, "Engineering flows in small devices: Microfluidics toward a lab-on-a-chip," Annu. Rev. Fluid Mech. **36**, 381 (2004).
[2] T. Bayraktar and S. B. Pidugu, "Characterization of liquid flows in microfluidic systems," Int. J. Heat Mass Transfer **49**, 815 (2006).
[3] R. F. Probstein, *Physiochemical Hydrodynamics*, 2nd ed. (Wiley, New York, 1994).
[4] C. L. Rice and R. Whitehead, "Electrokinetic flow in a narrow cylindrical capillary," J. Phys. Chem. **69**, 4017 (1965).
[5] H. K. Tsao, "Electroosmotic flow through an annulus," J. Colloid Interface Sci. **225**, 247 (2000).
[6] C. Yang and D. Q. Li, "Analysis of electrokinetic effects on the liquid flow in rectangular microchannels," Colloids Surf., A **143**, 339 (1998).
[7] Y. L. Zhang, T. N. Wong, C. Yang, and K. T. Ooi, "Electroosmotic flow in irregular shape microchannels," Int. J. Eng. Sci. **43**, 1450 (2005).
[8] X. C. Xuan and D. Q. Li, "Electroosmotic flow in microchannels with arbitrary geometry and arbitrary distribution of wall charge," J. Colloid Interface Sci. **289**, 291 (2005).
[9] L. B. W. Jolley, *Summation of Series* (Dover, New York, 1961).
[10] Q. Yi, K. H. Jeong, and L. P. Lee, "Theoretical and experimental study towards a nanogap dielectric biosensor," Biosens. Bioelectron. **20**, 1320 (2005).
[11] L. Pearson and D. R. S. Cumming, "Towards nano-fluidics by solvent deformation of electron beam resist," J. Vac. Sci. Technol. B **23**, 2793 (2005).
[12] S. Bhattacharyya, Z. Zheng, and A. T. Conlisk, "Electroosmotic flow in two-dimensional charged micro- and nano-channels," J. Fluid Mech. **540**, 247 (2005).
[13] M. Abramowitz and I. A. Stegun, *Handbook of Mathematical Functions* (Dover, New York, 1965).